This is the author's final, peer-reviewed manuscript as accepted for publication (AAM). The version presented here may differ from the published version, or version of record, available through the publisher's website. This version does not track changes, errata, or withdrawals on the publisher's site.

Nonadiabatic dynamics of polaron hopping and coupling with water on reduced TiO_2

Zhong-Fei Xu, Chuan-Jia Tong, Ru-tong Si, Gilberto Teobaldi, Li-Min Liu

Published version information

Citation: Z Xu et al. 'Nonadiabatic dynamics of polaron hopping and coupling with water on reduced TiO_2.' J Phys Chem Lett 13, no. 3 (2022): 857-863.

DOI: 10.1021/acs.jpclett.1c04231

This document is the Accepted Manuscript version of a Published Work (citation above) copyright © American Chemical Society after peer review and technical editing by the publisher. To access the final edited and published work see DOI above.

Please cite only the published version using the reference above. This is the citation assigned by the publisher at the time of issuing the AAM. Please check the publisher's website for any updates.

This item was retrieved from **ePubs**, the Open Access archive of the Science and Technology Facilities Council, UK. Please contact epublications@stfc.ac.uk or go to http://epubs.stfc.ac.uk/ for further information and policies.

Non-adiabatic Dynamics of Polaron Hopping and Coupling with Water on Reduced TiO_2

Zhong-Fei Xu[1,2,3], Chuan-Jia Tong[4], Ru-tong Si[3], Gilberto Teobaldi[5,6], Li-Min Liu[* 2]

1. College of Environmental Science and Engineering, North China Electric Power University, Beijing, 102206, P.R. China

2. School of Physics, Beihang University, Beijing 100191, P.R. China

3. Beijing Computational Science Research Center, Beijing 100193, P.R. China

4. School of Physics and Electronics, Central South University, Changsha 410083, P.R. China

5. Scientific Computing Department, STFC UKRI, Rutherford Appleton Laboratory, Harwell Campus, OX11 0QX Didcot, United Kingdom

6. School of Chemistry, University of Southampton, Highfield, SO17 1BJ Southampton, United Kingdom

[*]Corresponding author: liminliu@buaa.edu.cn

Abstract

By interplay between first principles molecular dynamics and non-adiabatic molecular dynamics simulations based on the decoherence-induced surface-hopping approach, we investigate and quantify the mechanisms through which different electron polaron hopping regimes in the reduced anatase TiO_2(101) surface influence recombination of photogenerated charge carriers, also in the presence of adsorbed water (H_2O) molecules. The simulations reveal that fast hopping regimes promote ultrafast recombination of photogenerated charge-carriers. Conversely, charge recombination is delayed in the presence of slower polaron hopping and even more so if the polaron is pinned at one Ti-site, as typical following adsorption of H_2O on the anatase(101) surface. These trends are related to the observed enhancement of the space and energy overlap between conduction band minimum and polaron band gap states, and the ensuing non-adiabatic couplings (NAC) strengths, during a polaronic hop. We expect these insights on the beneficial role of polaron diffusion pinning for the extended lifetime of photoexcitations in TiO_2 to sustain ongoing developments of photocatalytic strategies based on this substrate.

Key words

TiO_2, Polaron, Non-adiabatic dynamics, electron-phonon coupling

TOC Figure

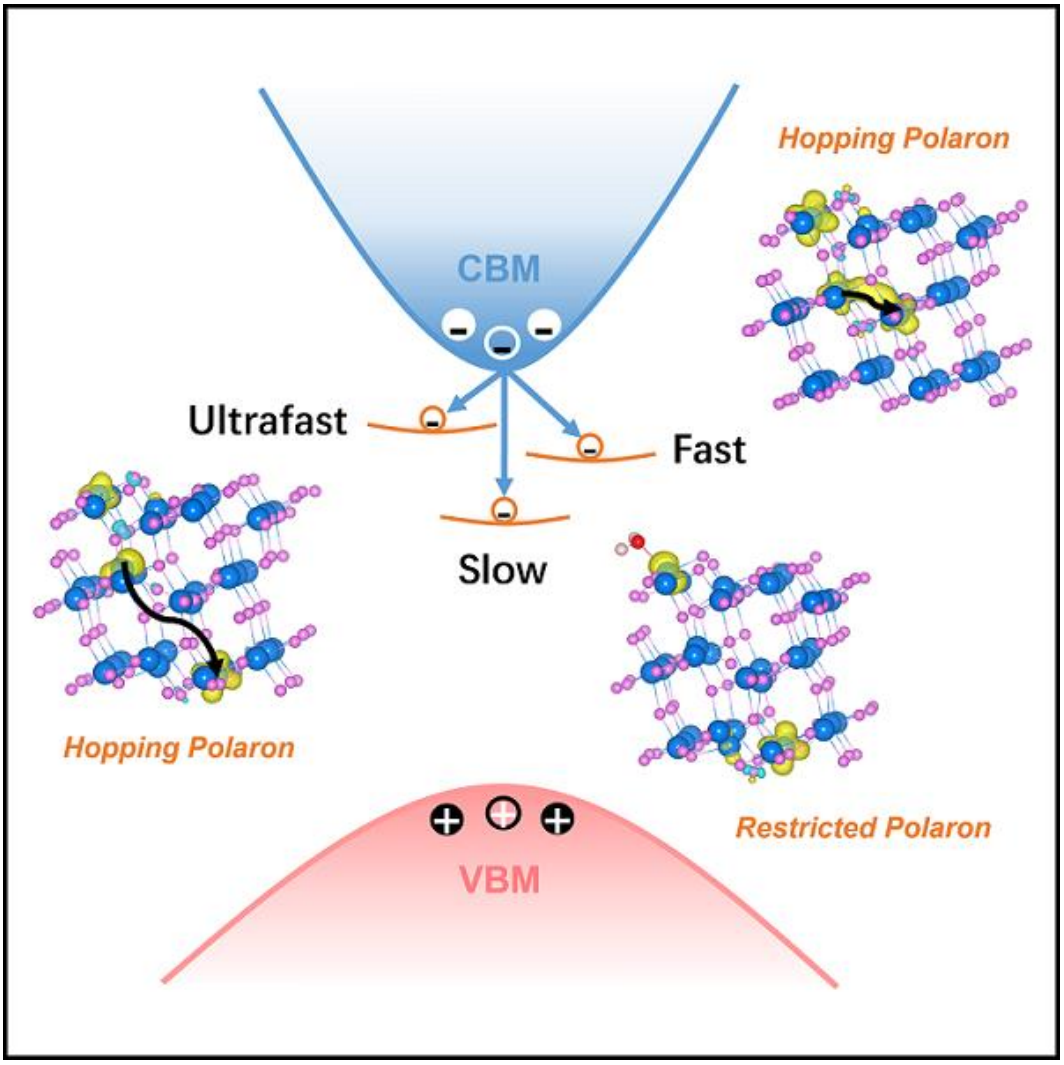
Hopping Polaron
CBM
Ultrafast
Fast
Slow
Hopping Polaron
Restricted Polaron
VBM

TiO_2 is a well-known photocatalyst that has found wide applications across many different fields[1-3]. Polarons, quasi-particles defined as trapped electrons (holes) coupled with the surrounding lattice distortion, invariably contribute to the physical properties and chemical reactivity of TiO_2 systems[4-6]. Different polaron behaviors have been found in the anatase and rutile TiO_2 phases, and related to the small, yet non-negligible, structural variations in the two polymorphs[7]. Point-defects such as oxygen vacancies and adsorbed or substitutional hydrogen on the rutile TiO_2(110) surface result in shallow donors and tend to form small polarons, experimentally located at about 1 eV below the conduction band minimum (CBM)[8].

Water (H_2O) dissociation and excess trapped electrons are observed in aqueous (101) interfaces in anatase TiO_2, with the behavior of the excess electrons being strongly dependent on the exposed surface, environment and electron donor properties[9]. Interstitial Ti atoms tend to diffuse from deep subsurface layers towards the surface as water or methanol is adsorbed on the TiO_2(110) surface, resulting in the enhancement of photo-absorption in reduced TiO_2 samples[10]. In anatase TiO_2, adsorption of H_2O can promote effective proton-diffusion by reducing the polaron-proton coupling, consistent with the experimental results[11]. Since the electronic properties and reactivity of polarons are strongly influenced by the crystal lattice and the presence of adsorbed species, further development of TiO_2-based systems requires investigation and understanding of the response of this quasi-particle to surface functionalization.

Photoexcited processes in solid-state systems are extremely challenging for simulation-based characterization because of the high computational costs needed for a description of the non-adiabatic process[12-14]. Surface hopping has increased in popularity because of the favorable compromises between accuracy of the results and computational cost[15, 16], which has been extensively applied to study photoexcited processes thanks to the robust accuracy and low computational cost of the methods and approximation used. For example, its application to $MAPbI_3$ has shown that the iodine anion vacancy leads to minor changes in the charge-carrier lifetime, which in turn is beneficial for the photocatalytic performance of the materials by comparison to neutral iodine and iodine cation vacancies[17]. Synergy of ion migration and charge carrier recombination has been found in $MAPbI_3$, with the iodide vacancy demonstrated to be the non-radiative charge recombination center[18]. Localization of impurity-phonon modes in differently doped rutile TiO_2 is the main factor that determines the electron-hole (e-h) recombination[19]. The approach has also been used to investigate the effects of polarons on charge-transfer α-Fe_2O_3. The simulations uncover that the neighboring Fe-Fe distance is the main driving force for the electron polaron hopping, which occurs by the adiabatic charge-transfer mechanism in this material[20].

The polaron usually diffuses at the room-temperature between the different sites. Thus it is vital to know how the polaron diffusion affect the carrier life and related properties. The simulation of TiO_2 brookite indicate that hole migration presents a small polaron character with band-like diffusion, and subsequent re-trapping. In contrast, hole polaron diffusions in anatase and TiO_2-B is found to take place via combination of short hops and re-trapping events[21]. The dynamics of small

polarons induced by photoexcitation at different temperatures in rutile TiO_2 have also been investigated, uncovering that polaron migration between Ti atoms is strongly correlated with quenching through an electron-hole recombination[22]. Although the motion of polarons is closely related to the photo-excited properties, the influence of different polaron hopping regimes on charge carrier recombination is yet to be studied systematically and understood quantitatively.

To start filling this gap, here we investigate and quantify the mechanisms through which different polaron hopping regimes can influence charge-recombination in defective TiO_2 systems, specifically the anatase TiO_2(101) surface with one oxygen vacancy (V_O) used to introduce two Ti^{3+} ions which, once coupled with the Ti-O polyhedrons, form two electron-polarons. More specifically, we explore and quantify the mechanisms through which the electron polaron mobility in anatase TiO_2(101), and the ensuing time-dependent changes in real-space and energy overlap between band-edges and polaron gap states as well as non-adiabatic couplings (NACs), affect the rate of recombination for photogenerated charge carries, also in the presence of adsorbed water (H_2O) molecules. Combination of first principles molecular dynamics (FPMD) and Non-adiabatic Molecular Dynamics (NAMD) simulations based on the decoherence-induced surface-hopping (DISH) approach reveal a direct and strong correlation between the rate of polaron mobility and excited state charge recombination, with processes capable of pinning polarons (e.g. H_2O adsorption) shown to significantly enhance the lifetime of photogenerated charge-carriers.

Computational methods

The first-principles molecular dynamics (FPMD) and electronic structure simulations of TiO_2 were performed using Density Functional Theory within the Perdew-Burke-Ernzerhof parameterization of the generalized gradient approximation (GGA), as implemented in the Vienna Ab initio Simulation Package (VASP) code[23]. The projector augmented wave (PAW) method was employed to describe electron-ion interactions[24]. For Brillouin zone (BZ) sampling, we used a grid of 3×3×1 k-points. The plane-wave basis cut-off was 400 eV. The convergence thresholds for total energies and atomic forces were 1×10^{-4} eV and 1×10^{-2} eV/Å, respectively. The anatase TiO_2(101) slab was constructed with three Ti-O layers and a 15 Å vacuum buffer to prevent interactions between adjacent surfaces. Spin-polarized local density approximation calculations were carried out with (isotropic) Hubbard corrections PBE+U_{eff} [24, 25] on the Ti d electrons (U_{eff} = 3.9 eV). The DFT-D3 method with Becke-Jonson damping was used for the description of van der Waals interactions[26, 27]. The systems are brought to 400 K by heating for 1 ps and then 5 ps trajectories with 1fs time step are generated in MD simulations. Non-adiabatic Molecular Dynamics (NAMD) calculations were performed using the decoherence-induced surface-hopping (DISH) approach[28], as implemented in the PYXAID package[15, 16].

The initial oxygen vacancy was introduced at the subsurface as discussed in the previous

works[29, 30]. Figure 1(a) shows the crystal structure of the (101) surface of anatase TiO_2 with one Vo (Vo-TiO_2). The polaron distribution and hopping regimes are analyzed on the basis of 5 ps MD simulations. The colored tetrahedrons mark the trapping sites (Ti_{5c}-L1, Ti_{5c}-L2, Ti_{5c}-L3, Ti_{5c}-L4) of the polaron during the MD simulations. At the start of the MD trajectory, the two polarons are located at the Ti_{5c}-L1 and Ti_{5c}-L3 sites, as shown in Figure 1(b) at 1 fs. The movies of polaron hopping are displayed in the Supporting Information, whereas one polaron is found to be restricted at the surface Ti_{5c}-L1 site throughout the MD trajectory, the other is observed to hop twice in 5 ps. Figure 1 (b) presents some typical point from the overall MD trajectory. The calculated diffusion path for this second subsurface polaron is Ti_{5c}-L3→Ti_{5c}-L2→Ti_{5c}-L4. This path can in turn be separated into two regimes depending on the short (*intensive hopping*) or long (*mild hopping*) time-delay between separated polaron hopping events. As shown in the upper panel of Figure 1(b), in the first, mild hopping stage the polaron transfers around Ti_{5c}-L3 and Ti_{5c}-L2 over 400 fs - 500 fs to finally hop to Ti_{5c}-L2 in 1060 fs - 1100 fs. The polaron then quickly hops back and forth (two hops with ~20 fs residence time, see the movies see the movies in supporting information) between Ti_{5c}-L2 and Ti_{5c}-L4 in 2065 fs -2139 fs, to eventually end at the Ti_{5c}-L4 site. The charge densities on other Ti atoms exhibits the delocalization characteristic of polaron.

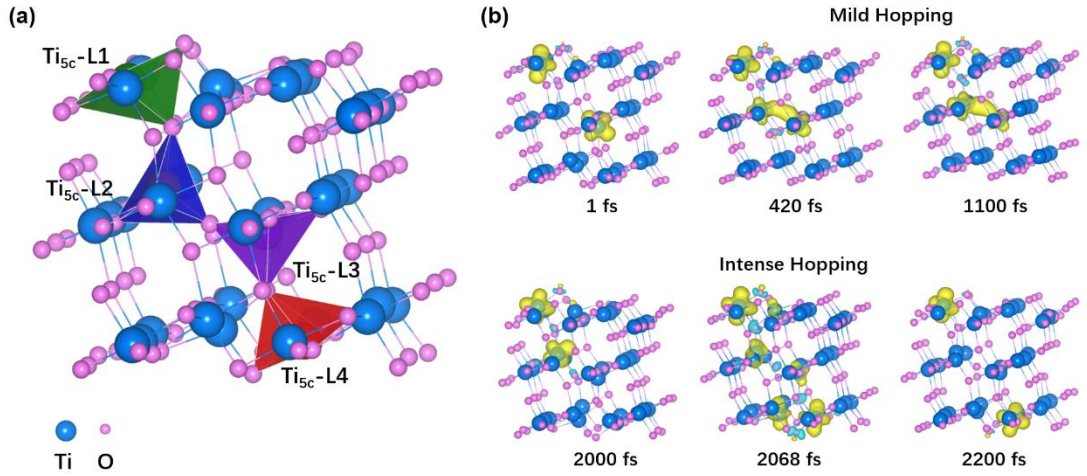

Figure 1. (a) Crystal structure of the anatase TiO_2 (101) surface. Blue and pink balls represent Ti and O atoms, respectively. The green, dark blue, purple, and red tetrahedrons mark the Ti_{5c}-L1, Ti_{5c}-L2, Ti_{5c}-L3, and Ti_{5c}-L4 polaron location in the MD simulations. (b) Time-evolution of the polaron charge-density (yellow color) at 1 fs, 420 fs, 1100 fs, 2000 fs, 2068 fs, and 2200 fs.

Lifetime is primarily used to characterize the time-scale of charge recombination, which in turn is primarily governed by the non-adiabatic couplings (NACs), $d_{jk} = \left\langle \varphi_j \middle| \frac{\partial}{\partial t} \middle| \varphi_k \right\rangle = \frac{\left\langle \varphi_j \middle| \nabla_{RH} \middle| \varphi_k \right\rangle}{\epsilon_k - \epsilon_j} \dot{R}$. NACs depends on the energy difference between the two non-adiabatically coupled electronic states $(\epsilon_k - \epsilon_j)$, the electron-phonon coupling matrix element $\left\langle \varphi_j \middle| \nabla_{RH} \middle| \varphi_k \right\rangle$, and the nuclear velocity $\dot{R}$.

To explore the influence of polaron motion on the charge carrier recombination in photoexcited processes for the studied system, Figure 2 compares the time evolution of the polaron location,

single-particle band-energies, and NACs in both the mild and intense polaron hopping. Figure 2(a)-(b) reports the previously discussed different regimes of polaron hopping: the mild (1020 fs - 1120 fs) and intense (2050 fs - 2150 fs) one. The results from the full 5 ps MD trajectory are showed in Figure S1. As seen in Figure 2(c), the mild polaron hopping regime results in no major oscillations of the CBM, polaron gap states and VBM, which indicates weak interaction between these electronic states.

However, as shown in Figure 2(d), huge energy oscillations for the CBM, VBM and polaron gap states appear in the intense polaron hopping regime. The energy resonance of these bands illustrates strong coupling, especially between the CBM and the polaron gap states. The strength of the NAC mainly relates to the phonon excitation and electron-phonon coupling. Larger NAC values usually indicate shorter lifetimes for charge carriers. The maximum NAC between the CBM and the polaron gap states for the mild hopping regime in Figure 2(e) is about 15 meV. Substantially larger NAC strengths of up to nearly 200 meV and -300 meV are conversely found in the intense polaron hopping regime (Figure 2(f)). The observed sudden spikes in the NAC values are testament to the significant electron-phonon coupling in the period of intense polaron hopping.

Based on these results, it can be predicted that the lifetime for the photoexcited electron in the intense polaron hopping regime will be much smaller than for the mild polaron hopping stage. This in turn suggest that activated polaron motion will promote the recombination of charge carriers. In addition, the oxygen atoms nearby the subsurface vacancy slightly moves towards the defect point during 1753 fs - 2065 fs. However, this kind of oxygen displacement mainly influences the phonon excitation properties.

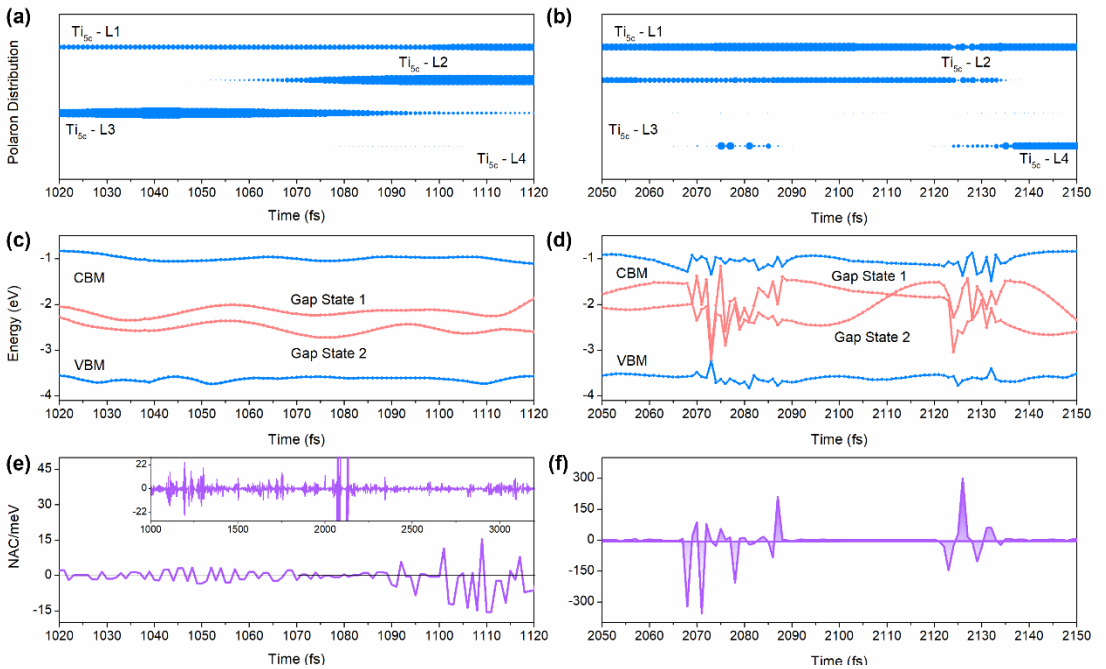

Figure 2. (a) The polaron location, (c) band-energy, and (e) NAC of the mild polaron hopping stage from 1020 fs to 1120 fs. (b) The polaron location, (d) band-energy, and (f) NAC of the intense polaron hopping stage from 2050 fs to 2150 fs.

The carrier recombination lifetime, τ, is calculated by fitting the short-time linear approximation to the exponential decay, $f(t)=\exp(-t/\tau)\approx 1-t/\tau$. Smaller lifetimes usually indicate faster charge recombination. As shown in Figure 3(a), we calculated the lifetime of the photoexcited electron relaxing from the CBM to the polaron gap state for different regimes of polaron hopping. We find that the electron relaxation behavior can be divided into several regimes: (i) 0 fs - 400 fs and 4100 fs - 5000 fs, with a lifetime of τ_1=352.2 ps and $\tau_{1'}$=321.5 ps corresponding to the polaron restricted at the Ti site. (ii) 4000 fs- 1200 fs, with a lifetime of τ_2=85.8 ps in the presence of mild polaron hopping. (iii) 2065 fs – 2727 fs, with a lifetime of τ_3=1.6 ps in the presence of intense polaron hopping with a polaron residence time of about 20 fs. It should be noted that one polaron prefers to stay at the surface and the other stays at the subsurface[31]. The initial distribution of the polaron may slightly affect the lifetime of the polarons. Otherwise, a delay region of the lifetime is found after hopping action is finished, which may relate to the variations of surrounding lattice structures. In order to know whether the number of the TiO_2 layers affect the conclusions observed here, another first-principles molecular dynamics were also carried out for 4 ps at 400 K. As shown in Figure S2 and S3, the results also indicated that the polaron hopping could observed between Ti_{5c}-L3' and Ti_{5c}-L2' in the first 1000 fs and then finally hops from Ti_{5c}-L3' to Ti_{6c}-L4' in 1550 fs - 1600 fs. The polaron hopping decrease the carrier lifetime, as found in the three-layer TiO_2. Further the water coverage and the functional may also affect the polaron hoping, while the finding of the polaron hopping should not be affected [7, 9, 32, 33]. To know the extent of this effect, some further works should be carried out. In order to determine whether the simulation time of 5 ps is longer enough, another simulations were carried out for 7ps. The corresponding result is shown in Fig. S4, and the same trend was shown for 5 ps and 7 ps.

Figure 3(b) gives enlarged pictures of the boundaries between the three regimes. Clearly, the kind of polaron hopping does influence the lifetime of the photoexcited electron. While intense polaron hopping leads to fast decay of the electron from CBM to polaron gap state, mild polaron hopping result in longer lifetimes. The lifetime for the restricted polaron is nearly four and two hundred times longer than for the mild and intense hopping polarons, respectively.

To identify the reason behind such a huge difference in the lifetime depending on the polaron hopping regime, we turn to the overlap between energy bands (Figure 3(c)). It can be seen that the overlap between the CBM and the polaron gap state is much larger during a polaron hop and accompanied by instantaneous increase of the NAC-strength. Especially, for the fast, intense polaron hopping regime (2068 fs), an extended overlap between the charge-density of the CBM and the polaron gap state is found. This reflects the increased NAC coupling and long quantum coherence time between the CBM and the polaron gap state. These results indicate that fast, intense polaron hopping is associated with stronger NACs and large charge density overlaps, resulting in accelerated charge carrier recombination.

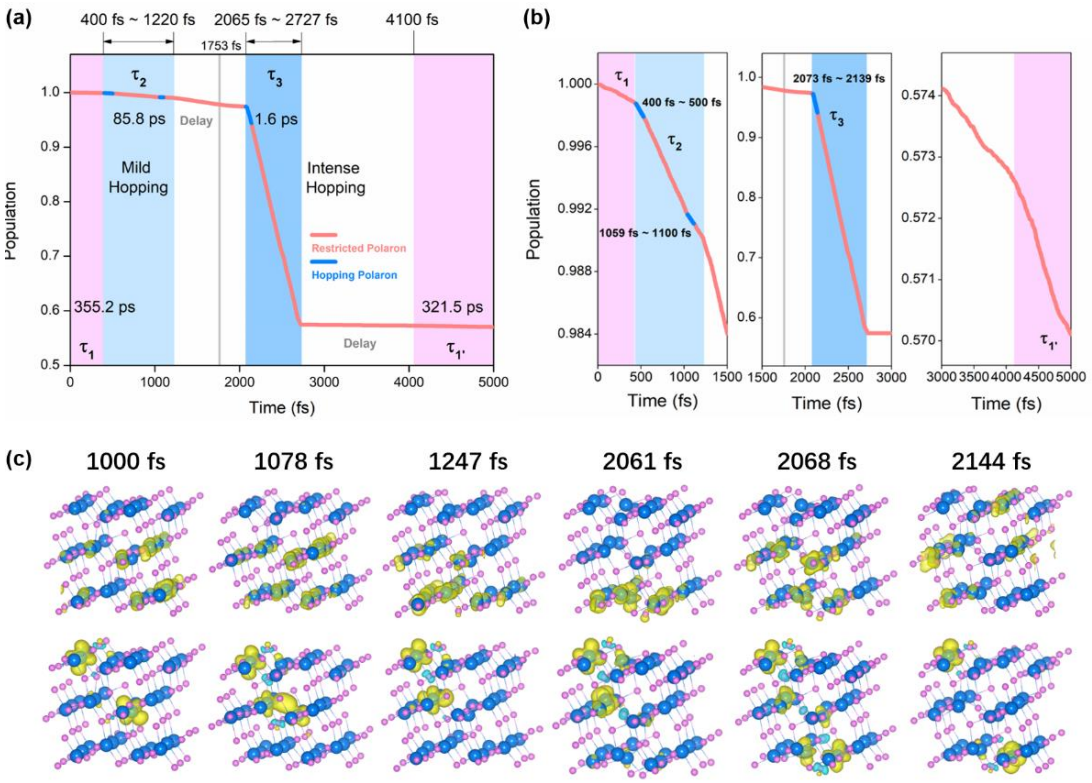

Figure 3. (a) Time-evolution of the photoexcited electron relaxation from the CBM to the polaron gap state. Blue line segments are the polaron hopping regimes. Panel (b) reports a close up around the different regimes with different lifetimes ($\tau_{1\text{-}4}$, $\tau_{1'}$). (c) Time-evolution of the charge density of the CBM (upper panels) and polaron gap state (lower panels) (yellow color). The pink and blue balls stand for the O and Ti atoms.

Since the polaron hopping behavior mainly relates to the strength of phonon-electron coupling and lifetime of charge carriers, we calculated the distortion of the TiO polyhedrons to characterize the lattice vibrations that can be recognized as phonon coupling with the excess electrons at the special sites. Figure 4 (a) reports the distortion (ζ) of the Ti-O bond lengths for the Ti_{5c}-L1, Ti_{5c}-L2, Ti_{5c}-L3, and Ti_{5c}-L4 sites, calculated as $\zeta = (\sum_{i=1}^{n}|d_i - d_{mean}|)/5$. d_{mean} is the average bond length of Ti-O in prinstine anatase TiO_2, n is the coordination number of the Ti atoms. The results are smoothed as the bold curve shows in Figure 4(a).

The distortion of the restricted polaron at the Ti_{5c}-L1 site remains almost unchanged throughout the 5 ps MD trajectory. The distortion of Ti_{5c}-L3 changes minimally too during the MD trajectory, even when the polaron hops to Ti_{5c}-L2. However, the distortion of the Ti_{5c}-L2 site is clearly enhanced around 1200 fs, to eventually recover the original values at around 2000 fs, when the distortion for the Ti_{5c}-L4 site changes abruptly due to the polaron hopping to this site. The gradual variation of the locate structure for Ti_{5c}-L2 may contribute to the extended lifetime observed in Figure 3(a) and the observed mild polaron hopping from Ti_{5c}-L3 to Ti_{5c}-L2. The suddenly increased distortion for Ti_{5c}-L4 around 2000 fs agrees well with the corresponding intense hopping behavior, and the resultant drop of lifetime for photogenerated charge-carriers. The distortion of Ti_{5c}-L4 then

keeps larger values as polaron has restricted on this site.

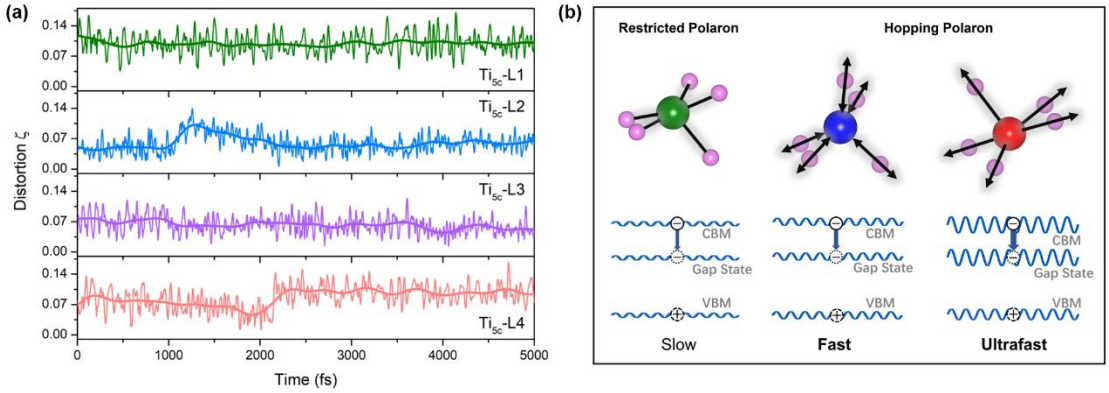

Figure 4. (a) The distortion ζ of the TiO Ti_{5c}-L1, Ti_{5c}-L2, Ti_{5c}-L3, Ti_{5c}-L4 polyhedrons. The bold line is the smoothed curve by Fast Fourier Transformation (FFT) method with 150 pts. (b) Schematic representation of the influence of the polaron environment on electron-phonon coupling and hopping lifetimes.

Our results indicate that different polaron hopping regimes, with different electron-phonon coupling strengths, will lead to different recombination for photoexcited polarons. Intense polaron hopping result in ultrafast charge recombination whereas mild polaron hopping result in slower charge-recombination albeit substantially faster than for the restricted polaron case. Based on these results, in Figure 4(b) we propose a schematic representation of the influence of the polaron environment on electron-phonon coupling and hopping lifetimes.

Previous studies have shown that in photocatalytic processes on TiO_2 water (H_2O) molecules invariably drive electron polaron diffusion to the surface[10]. These results prompt for extension of our investigation to the role of H_2O adsorption, and its documented effects on polaron diffusion, for the lifetime of photogenerated charge-carrier in the defective anatase (101) surfaces. Figure S5 reports the calculated time-evolution of the polaron location, band-energies, and NACs values for Vo-TiO_2 in the presence of one adsorbed H_2O molecule (H_2O-Vo-TiO_2). As expected, both electron polarons remain at the Ti_{5c}-L1 and Ti_{5c}-L4 sites. Over the full (4 ps) MD trajectory, no motion of polarons is observed, indicating that the H_2O molecule if highly effective in limiting polaron hopping to prevent the ultrafast and fast recombination of charge carriers in the photocatalytic processes. As we discussed above, and shown in Figure S6, restricted polarons have little influence on the electronic structure and nonadiabatic properties.

In order to further quantify the role of the adsorbed H_2O molecule for the lifetime of the photoexcitations, in Figure 5 we compare the dephasing times, spectral densities and normalized autocorrelation functions (ACFs) for Vo-TiO_2 and H_2O-Vo-TiO_2. The lifetimes for the two systems are nearly the same albeit with a slightly larger value for Vo-TiO_2. These results confirm small effects due to H_2O on the non-adiabatic properties of the defective Vo-TiO_2 system. The phonon related pure-dephasing time is calculated from the ACF of the energy gap fluctuation along the MD trajectory, which affects the de-coherence time. The initial value of the unnormalized ACF is the

squared standard deviation, which represent the average fluctuation in energy gap. In general, the larger initial value, slower and more asymmetric decay of the unnormalized ACF lead to faster dephasing. As shown in Figures 5(b) and (c), pure the dephasing times for Vo-TiO_2 (5.04 fs) and H_2O-Vo-TiO_2 (4.74 fs) are rather similar. The initial value of the unnormalized ACF for Vo-TiO_2 and H_2O-Vo-TiO_2 is 0.0439 and 0.0496, respectively. Fourier transform of the normalized ACF gives the frequency of the vibrational modes which contribute to the decay of the ACF, leading to the phonon influence spectrum shown in Figure 5(d). The similarity between the phonon modes calculated for Vo-TiO_2 and H_2O-Vo-TiO_2 is indicative of comparable electron-vibrational interactions in two systems. These phonon modes are consistent with the results observed experimentally[34, 35]. The calculated very contained differences for Vo-TiO_2 and H_2O-Vo-TiO_2 reiterate that adsorption of H_2O mainly act to restrict polaron motion, which is beneficial for the photocatalytic processes owing to the ensuing increase of the lifetime for photogenerated charge-carrier (Figure 3).

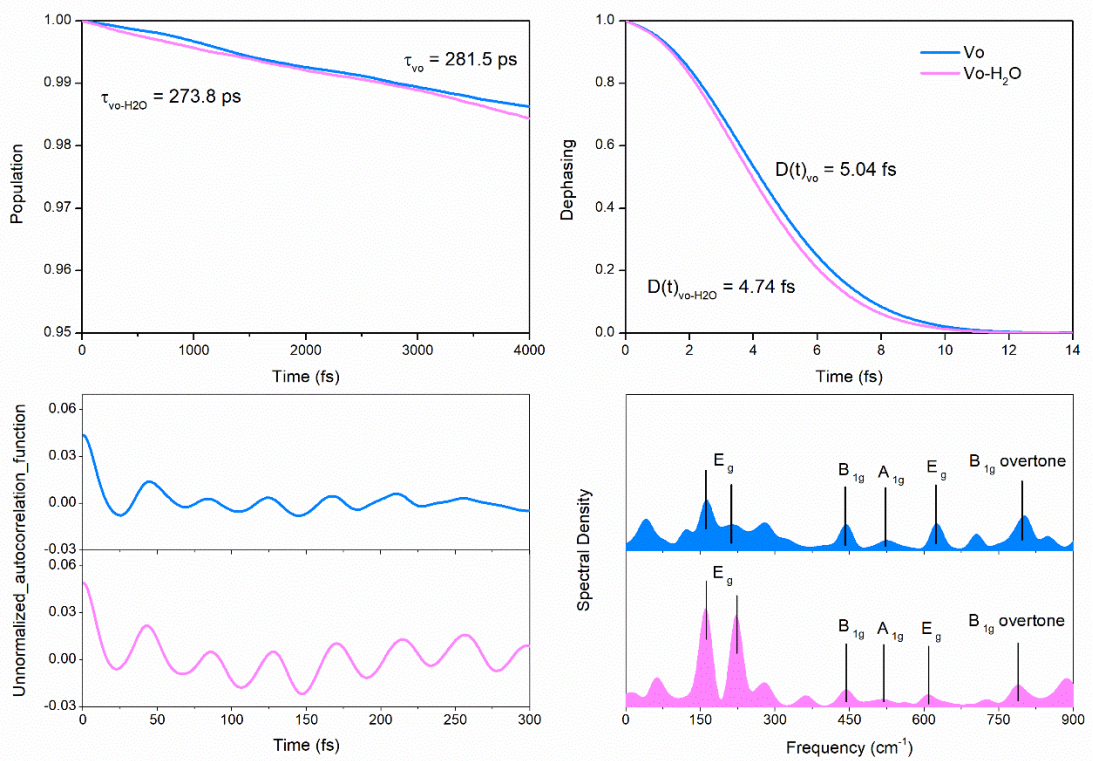

Figure 5. (a) Lifetime, (b) pure-dephasing time, (c) unnormalized autocorrelation function, (d) spectral density of Vo-TiO_2 and H_2O-Vo-TiO_2. Insert pictures of (a) are corresponding atomic structures and polarons (yellow color). The pink and blue balls stand for the O and Ti atoms. The hydrogen and oxygen atoms of water were shown in white and red colors.

In conclusion, we have investigated the mechanisms through which polaron hopping affects non-adiabatic properties in defective anatase TiO_2(101). The simulations uncover clear relationships between the rate of polaron hopping and the oscillations in band-energies as well as in the non-adiabatic couplings (NACs). Specifically, we find fast (intense) hopping regimes to promote ultrafast recombination of photogenerated charge-carriers. In contrast, charge recombination is

progressively slowed in the presence of slower (mild) polaron hopping and even more so if the polaron hopping is absent and the polaron resides at just one Ti-atom for long-timescales. The simulations reveal the details through which the space and energy overlap between conduction band minimum and polaron band gap states, and the ensuing NAC-strengths, are increased during a polaronic hop. It is found that the distortion of the TiO polyhedrons along the MD trajectory is a key factor for the charge recombination rate, with the intense and mild polaron hopping regimes being characterized by abrupt and gradual increases in the TiO distortion, respectively. Consistent with the result that polarons of restricted mobility are beneficial to prevent charge recombination, the simulations confirm that adsorbed H_2O molecules, and their polaron-pinning effect, are also effective in extending the lifetime of photogenerated charge carriers in anatase TiO_2(101). We expect these insights on the interplay between polaron hopping and surface functionalization for the relaxation of photoexcitations at the anatase (101) surface to provide a valuable and timely contribution to ongoing developments in the field of TiO_2-based photocatalysis.

This work was financially supported by the National Natural Science Foundation of China (11974037，U1930402), and the Key Science and Technology Research Project of Yunnan (202002AB080001-1-6 and 202102AB0800008). G.T. and L.M.L. acknowledge support by the Royal Society Newton Advanced Fellowship scheme (grant No. NAF\R1\180242). We are grateful to the Beihang HPC and Tianhe2-JK for generous grants of computer time. We are also grateful for technical support from the High Performance Computing Center of Central South University.

The polaron location, energy evolution, NAC of Vo-TiO_2 (Both hopping and restricted polaron, and H_2O-Vo-TiO_2. The polaron location and lifetime evolution of four layer Vo-TiO_2.

[1] K. Hashimoto, H. I. and A. Fujishima, TiO_2 Photocatalysis: A Historical Overview and Future Prospects, *Jan. J. Appl. Phys.*, **2005**, 44 (12), 8269-8285.

[2] J. Schneider, M. Matsuoka, M. Takeuchi, J. L. Zhang, Y. Horiuchi, M. Anpo, and D. W. Bahnemann, Understanding TiO_2 Photocatalysis: Mechanisms and Materials, *Chem. Rev.*, **2014**, 114(19), 9919-9986.

[3] A. J. Tanner, B. Wen, J. Ontaneda, Y. Zhang, R. Grau-Crespo, H. H. Fielding, A. Selloni, and G.Thornton, Polaron-Adsorbate Coupling at the TiO_2 (110)- Carboxylate Interface, *J. Phys. Chem. Lett.*, **2021**, 12(14), 3571-3576.

[4] M. Reticcioli, U. Diebold, G. Kresse, C. Franchini, Small Polarons in Transition Metal Oxides. In: Andreoni W., Yip S. (eds) Handbook of Materials Modeling. Springer, Cham. **2019**

[5] B. X. Yan, D. Y. Wan, D. Y. Wan, X. Chi, C. J. Li, M. R. Motapothula, S. Hooda, P. Yang, Z. Huang, S. W. Zeng, A. G. Ramesh, S. J. Pennycook, A. Rusydi, Ariando, J. Martin, and T. Venkatesan, Anatase TiO_2-A Model System for Large Polaron Transport, *ACS Appl. Mater. Interfaces*, **2018**, 10(44), 38201-38208

[6] G. Kolesov, B. A. Kolesov, and E. Kaxiras, Polaron-induced Phonon Localization and Stiffening in Rutile TiO_2, *Phys. Rev. B*, **2017**, 96, 195165.

[7] M. Setvin, C. Franchini, X. F. Hao, M. Schmid, A. Janotti, Merzuk. Kaltak, C. G. Van de Walle, G. Kresse, and U. Diebold, Direct View at Excess Electrons in TiO_2 Rutile and Anatase, *Phys. Rev. Lett.*, **2014**, 113, 086402.

[8] P. G. Moses, A. Janotti, C. Franchini, G. Kresse, and C. G. Van de Walle, Donor Defects and Small Polarons on the TiO_2 (110) Surface, *J. Appl. Phys.*, **2016**, 119, 181503.

[9] S. Selcuk and A. Selloni, Facet-dependent Trapping and Dynamics of Excess Electrons at Anatase TiO_2 Surfaces and Aqueous Interfaces, *Nature Materials*, **2016**, 15, 1107-1112

[10] B. Wen, W. J. Yin, A. Selloni, and L. M. Liu, Defects, Adsorbates, and Photoactivity of Rutile TiO_2 (110): Insight by First-Principles Calculations, *J. Phys. Chem. Lett.* **2018**, 9, 18, 5281-5287

[11] Y. N. Zhu, G. Teobaldi, and L. M. Liu, Water-Hydrogen-Polaron Coupling at Anatase TiO_2(101) Surfaces: A Hybrid Density Functional Theory Study, *J. Phys. Chem. Lett.* **2020**, 11, 4317-4325.

[12] P. Ehrenfest, Adiabatische Transformationen in der Quantentheorie und ihre Behandlung durch Niels Bohr, *Naturwissenschaften*, **1923**, 11, 543−550

[13] S. A. Fischer, C. T. Chapman, and X. S. Li, Surface Hopping with Ehrenfest Excited Potential, *J. Chem. Phys.* **2011**, 135, 144102.

[14] J. C. Tully, Molecular Dynamics with Electronic Transitions, *J. Chem. Phys.* **1990**, 93, 1061-1071.

[15] A. V. Akimov, and O. V. Prezhdo, The PYXAID Program for Non-Adiabatic Molecular Dynamics in Condensed Matter Systems, *J. Chem. Theory Comput.* **2013**, 9, 4959-4972

[16] A. V. Akimov, and O. V. Prezhdo, Advanced Capabilities of the PYXAID Program: Integration Schemes, Decoherence Effects, Multiexcitonic States, and Field-Matter Interaction, *J. Chem. Theory Comput.* **2014**, 10, 789-804.

[17] W.Li, Y. Y. Sun, L. Q. Li, Z. H. Zhou, J. F. Tang, and O. V. Prezhdo, Control of Charge Recombination in Perovskites by Oxidation State of Halide Vacancy, *J. Am. Chem. Soc.* **2018**, 140, 46, 15753-15763

[18] C. J. Tong, L. Q. Li, L. M. Liu, and O. V. Prezhdo, Synergy between Ion Migration and Charge Carrier Recombination in Metal-Halide Perovskites, *J. Am. Chem. Soc.* **2020**, 142, 6, 3060–3068

[19] L. L.Zhang, Q. J. Zheng, Y. Xie, Z. G. Lan, O. V. Prezhdo, Wissam A. Saidi, and Jin Zhao, Delocalized Impurity Phonon Induced Electron-Hole Recombination in Doped Semiconductors, *Nano Lett.* **2018**, 18, 1592-1599

[20] Z. H. Zhou, R. Long, and O. V. Prezhdo, Why Silicon Doping Accelerates Electron Polaron Diffusion in Hematite, *J. Am. Chem. Soc.* **2019**, 141, 20222-20233

[21] J. J. Carey, J. A. Quirk, and K. P. McKenna, Hole Polaron Migration in Bulk Phases of TiO_2 Using Hybrid Density Functional Theory, *J. Phys. Chem. C* **2021**, 125, 12441-12450

[22] L. L. Zhang, W. B. Chu, C. Y. Zhao, Q. J. Zheng, O. V. Prezhdo, and J. Zhao, Dynamics of Photoexcited Small Polarons in Transition-Metal Oxides, *J. Phys. Chem. Lett.* **2021**, 12, 2191−2198

[23] P. E. Bloch, Projector augmented-wave method, *Phys. Rev. B* **1994**, 50, 17953.

[24] J. P. Perdew, K. Burke, M. Ernzerhof, Generalized Gradient Approximation Made Simple, *Phys.*

Rev. Lett. **1996**, 77, 3865.

[25] A. I. Liechtenstein, V. I. Anisimov and J. Zaane, Density-functional Theory and Strong Interactions: Orbital Ordering in Mott-Hubbard Insulators, *Phys. Rev. B*, **1995**, 52, R5467.

[26] S. Grimme, J. Antony, S. Ehrlich, and S. Krieg, A Consistent and Accurate Ab Initio Parametrization of Density Functional Dispersion Correction (DFT-D) for the 94 Elements H-Pu, *J. Chem. Phys.* **2010**, 132, 154104.

[27] S. Grimme, S. Ehrlich, and L. Goerigk, Effect of the Damping Function in Dispersion Corrected Density Functional Theory, *J. Comp. Chem.* **2011**, 32, 1456.

[28] H. M. Jaeger, S. Fischer, Oleg V. Prezhdo, Decoherence-Induced Surface Hopping. *J. Chem. Phys.* **2012**, 137, 22A545.

[29] H. Z. Cheng and A. Selloni, Surface and Subsurface Oxygen Vacancies in Anatase TiO_2 and Differences with Rutile, *Phys. Rev. B*, **2009**, 79, 092101.

[30] Y. B. He, O. Dulub, H. Z. Cheng, A. Selloni, and U. Diebold, Evidence for the Predominance of Subsurface Defects on Reduced Anatase TiO_2 (101), *Phys. Rev. L*, **2009**, 102, 106105.

[31] H. Z. Cheng and A. Selloni, Energetics and Diffusion of Intrinsic Surface and Subsurface Defects on Anatase TiO_2 (101), *J. Chem. Phys.* **2009**, 131, 054703.

[32] C. M. Yim, J. Chen, Y. Zhang, B. J. Shaw, C. Pang, D. C. Grinter, H. Bluhm, M. Salmeron, C. A. Muryn, A. Michaelides and G. Thornton, Visualization of Water-induced Surface Segregation of Polarons on Rutile TiO_2 (110), *J. Phys. Chem. Lett.* **2018**, 9, 17, 4865.

[33] E. Finazzi, C. D. Valentin, G. Pacchioni and A. Selloni, Excess Electron States in Reduced Bulk Anatase TiO_2: Comparison of Standard GGA, GGA+U, and Hybrid DFT Calculations *J. Chem. Phys.*, **2008**, 129, 154113.

[34] H. Berger, H. Tang, F. Lévy, Growth and Raman Spectroscopic Characterization of TiO_2 Anatase Single Crystals. *J. Cryst. Growth*, **1993**, 130, 108.

[35] G. Cristian Vásquez, M. Andrea Peche-Herrero, David Maestre, Belén Alemán, Julio Ramírez-Castellanos, Ana Cremades,a José M. González-Calbet and Javier Piquerasa, *J. Mater. Chem. C*, **2014**, 2, 10377